Raman Fine Structure in Crystalline C_{60}: The Effects of Merohedral Disorder, Isotopic Substitution, and Crystal Field

P. J. Horoyski and M. L. W. Thewalt
Department of Physics, Simon Fraser University, Burnaby, British Columbia, Canada V5A 1S6

T. R. Anthony
GE Corporate Research & Development Center, General Electric Company, Schenectady, New York 12301
(Received 12 July 1994)

Richly structured intramolecular vibrational modes of crystalline C_{60} are observed using high-resolution Fourier-transform Raman spectroscopy. The narrow linewidths of these modes, as small as 0.1 cm^{-1}, reveal a wealth of detail below the 260 K fcc to sc transition. While clear evidence of crystal field splittings for both phases is observed, the majority of the low temperature splittings are unexpectedly found to result from the presence of merohedral disorder. Comparison of spectra from natural and ^{12}C enriched samples reveals that isotopic effects play a minor role, except for the $A_g(2)$ mode, which in the natural C samples has a complex structure quite different from that recently reported for isolated C_{60}.

PACS numbers: 78.30.Hv, 63.20.Hp, 81.30.Hd

The discovery [1] of the new "fullerene" allotropes of carbon, exemplified by C_{60} and soon followed by an efficient method for their synthesis [2], led to a burst of theoretical and experimental activity on their physical properties. Much of this activity concentrated on the vibrational properties of C_{60} and their elucidation by Raman scattering. Comparison between theory and experiment was greatly simplified by the high symmetry (I_h), resulting in only ten Raman active modes for the isolated molecule and the relative weakness of solid state effects, causing the crystalline C_{60} (c-C_{60}) Raman spectrum at low resolution to deviate only slightly from that expected for the isolated molecule. As a result, the coarser features of the c-C_{60} Raman spectrum are now well understood, and all of the vibrational mode energies have been determined [3–5].

Much less is known regarding the fine structure of the Raman lines, which has been ascribed to crystal field splittings of the degenerate molecular modes [3,6]. Another possibility would be isotopic effects, since C_{60} made from natural carbon contains 1.11% ^{13}C, and thus almost half of its molecules have one or more substitutions of ^{13}C for ^{12}C. Very recently such isotopic splittings have been observed for the ~1470 cm^{-1} $A_g(2)$ mode of presumably isolated natural C_{60} molecules in frozen CS_2 [7].

In this Letter we report a detailed study of the c-C_{60} fine structure using Fourier-transform Raman spectroscopy at resolutions of up to 0.02 cm^{-1}. A wealth of reproducible fine structure is observed, with components having linewidths as small as 0.1 cm^{-1} FWHM. While there is some evidence for "normal" crystal field splittings [3,6], we shall show that most of the fine structure is unexpectedly due to the merohedral orientational disorder [8]. An exception is the $A_g(2)$ mode, which in c-C_{60} (where we use this label to denote crystalline C_{60} made from natural carbon) shows a complex structure which is greatly simplified in a c-$^{12}C_{60}$ sample made from 99.95% ^{12}C. However, the $A_g(2)$ structure in c-C_{60} is entirely different from that reported earlier for C_{60} in CS_2 [7] and verified by us here. Thus the $A_g(2)$ fine structure in c-C_{60} must arise from some yet unexplained interplay of isotopic and solid state effects.

The c-C_{60} used in our initial studies was grown by vacuum sublimation of 99.9% (in terms of other fullerenes) C_{60} powder (Texas Fullerenes) as previously described [9]. The c-$^{12}C_{60}$ was similarly grown from $^{12}C_{60}$ powder produced in the usual manner [2] from ^{12}C pyrolytic graphite rods deposited from 99.95% ^{12}C methane (Cambridge Isotope Labs). Spectra were also collected from c-C_{60} produced from natural methane using the same process; no difference was found from the spectra observed in c-C_{60} grown from the commercial C_{60} powder. Mass spectroscopy revealed the expected 51% concentration of $^{12}C_{60}$ in the natural c-C_{60}, and 97.3% $^{12}C_{60}$ in the "pure" sample, consistent with the 99.95% ^{12}C content of the methane.

The Raman spectra were collected with a Bomem DA8.01 interferometer, with excitation from a line-narrowed Ti:sapphire laser (750 to 895 nm) or a Nd:YAG laser (1.064 μm). The samples were either immersed in liquid He or held at a controlled temperature in flowing He gas using a calibrated Si-diode temperature sensor. Scattered laser light was rejected using either holographic filters (Physical Optics Corp.) or atomic vapor filters [10]. The use of such longer wavelength excitation leads to large Raman signals due to the transparency of the samples and also eliminates problems related to sample heating and photodegradation [3,4]. The Raman fine structure details were independent of laser wavelength over the range used here.

 0031-9007/95/74(1)/194(4)$06.00

The temperature evolution of four representative gerade modes of c-C_{60} is shown in Fig. 1. As previously reported [3,6], there is little fine structure above the ~260 K first order phase transition, since in the fcc (T_h^3) high temperature phase the molecules are freely rotating and most crystal field effects are "smeared out." An exception is the ~273 cm^{-1} $H_g(1)$ mode, which is split into a doublet at 272.3 and 266.3 cm^{-1} (T = 261 K). Just below this temperature, the crystal is in the sc (T_h^6) low temperature phase, and two additional $H_g(1)$ components appear at 273.9 and 260.9 cm^{-1} (T = 259 K). The appearance and disappearance of these components revealed a hysteresis loop only 0.9 K in width centered at 259.9 K. As the temperature is lowered below 259 K, there is some reduction of the linewidths but the relative intensities of the four components remain constant. The $H_g(1)$ spectrum of c-C_{60} and c-$^{12}C_{60}$ are seen to be identical except for a small (0.11 cm^{-1}) shift to higher energy for all four c-$^{12}C_{60}$ components as might be expected from a $(m_1/m_2)^{1/2}$ effect. Since $H_g(1)$ is the lowest energy intramolecular mode, well separated in energy from the nearest silent mode [4,11], and since difference scattering is not possible at the lowest temperatures, all of these components can be attributed with certainty to the $H_g(1)$ mode. This $H_g(1)$ fine structure is entirely consistent with normal crystal field effects. The degenerate H_g modes in I_h symmetry can split into $E_g + F_g$ under T_h^3 symmetry and $A_g + 2E_g + 5F_g$ under T_h^6 symmetry. A recent theoretical calculation of the intramolecular phonons predicts a quartet for the $H_g(1)$ mode in the low T phase [11]. The zone center energies taken from Ref. [11], shifted up by 23 cm^{-1}, are indicated in Fig. 1 by four vertical arrows, in remarkably good agreement with the measured fine structure.

Next in Fig. 1 we see the spectrum of a weak feature at ~485 cm^{-1}, ascribed [4] to $G_g(1)$ (note that in c-C_{60} all gerade modes are Raman allowed, not just A_g and H_g, which are the only allowed modes for isolated C_{60}). As with the $H_g(1)$ mode, the $G_g(1)$ mode is fairly well removed in energy from any silent modes, allowing all of the fine structure centered at ~485 cm^{-1} to be attributed to it. Next to it is shown the ~774 cm^{-1} $H_g(4)$ mode. The $H_g(4)$ mode has a very strong Raman signal, and so all of the fine structure seen is labeled as components of the $H_g(4)$ mode, since it is unlikely that they arise from either activated ungerade modes or from combination modes, which are very much weaker. At first glance the behavior of the $G_g(1)$ and $H_g(4)$ modes appears similar to that of the previously described $H_g(1)$, in that fine structure appears below T = 260 K and becomes increasingly sharper at lower T.

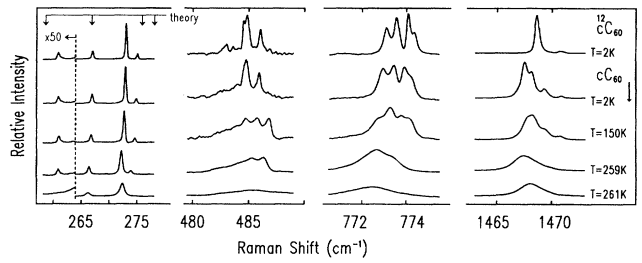

FIG. 1. Temperature evolution of the $H_g(1), G_g(1), H_g(4)$, and $A_g(2)$ (from left to right) Raman components of crystalline C_{60}. The spectra within each subsection of the energy axis are plotted on the same scale, but shifted for clarity. The top curve is the Raman spectrum of 97.3% $^{12}C_{60}$ crystals at 2 K, while the bottom four data sets are for c-C_{60} obtained from natural carbon. The 2 K spectra were taken from crystals which were slowly cooled through the ~85 K glass transition. Energies labeled "theory" for $H_g(1)$ are taken from Ref. [11], shifted up by 23 cm^{-1}.

A significant difference from $H_g(1)$, most obvious in Fig. 1 for the $G_g(1)$ mode, is that the relative intensities of the fine structure components show a significant temperature dependence between 260 and ~90 K, below which temperature they become constant. This immediately suggests a connection with the merohedral orientational disorder present in the sc phase, in which the four molecules in the unit cell have a preferred orientation with respect to their ⟨111⟩ axes which lowers the electrostatic interaction between the molecules, but at T $\gtrsim$ 90 K make thermally activated hops between this ground state configuration and another local minimum configuration which is only ~12 meV higher in energy [8,12,13].

The effects of this merohedral disorder, which freezes in on the laboratory time scale at ~85 K due to a ~260 meV activation barrier to the hopping, has previously been observed by its effects on x-ray scattering [8], thermal conductivity [12], and dilatometry [13]. Given the ~12 meV misorientation energy, ~17% of the molecules will be misoriented at low T if the sample is cooled slowly so that it enters the "glassy" state at ~85 K; a higher percentage of misorientations is possible by rapidly quenching the sample, which freezes in the disorder at a higher temperature. Note that the low temperature state shows merohedral disorder and is not truly in a glassy state, in that the molecules are still in distinct orientations, and not distributed over a range of orientations.

To test whether this merohedral disorder is involved in the suggestive temperature dependence of the relative intensities of the $G_g(1)$ and $H_g(4)$ (and many others) fine structure components, we have compared the T = 2 K Raman spectra of identical samples cooled at different rates, ranging from slowly cooling to 85 K over 12 h, to dropping small crystals directly from room temperature into superfluid He (samples were also quenched rapidly from ~220 to 2 K; no difference was found between these and samples quenched directly from room temperature, in which the crystals first pass through the fcc-sc transition).

As can be seen in Fig. 2, the quench rate has a major effect on the relative intensities of the $G_g(1)$ and $H_g(4)$ components at T = 2 K and also on the $A_g(2)$ doublet seen in c-$^{12}C_{60}$ (c-$^{12}C_{60}$ spectra are used in Fig. 2 since

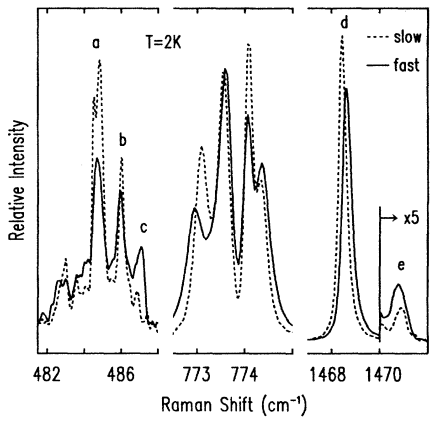

FIG. 2. $G_g(1), H_g(4)$ and $A_g(2)$ mode fine structure of 97.3% $^{12}C_{60}$ single crystals at $T = 2$ K as a function of the rate of cooling into the glassy state. The "fast" quench spectra have been scaled to the "slow" quench spectra by matching the intensities of the $A_g(1)$ vibrational mode which has no fine structure in either c-$^{12}C_{60}$ or c-C_{60}. The weak, high energy peaks in the $A_g(2)$ spectra have been multiplied by a factor of 5 for clarity. See text for an explanation of fast quench and slow quench.

the $G_g(1)$ and $H_g(4)$ components are sharper and there is less background; the pronounced isotopic effects on $A_g(2)$ seen in Fig. 1 will be discussed later). The quench rate dependence of the relative intensities at $T = 2$ K is exactly what one would expect from the disorder frozen in at $T = 85$ K (slow cooling) or $T \sim 115$ K (fast quench), based on the temperature dependence of the relative intensities observed above 85 K.

Further confirmation that this fine structure is due to the merohedral disorder comes from a more detailed study of the relative fine structure intensities between 85 and 250 K as shown in Fig. 3. The relative intensities of the $G_g(1)$ a vs b and b vs c components (as labeled in Fig. 2) vary with an activation energy of 11.2 and 12.2 meV, respectively, while the $A_g(2)$ doublet has an activation energy of 11.5 meV. Within our estimated accuracy of ± 2 meV, these values agree exactly with the previously determined [12,13] misorientation energies of ~ 12 meV.

The observation of sharp fine structure rather than broad bands is thus a consequence of the fact that the disorder is merohedral rather than truly glassy: Even in the disordered state only certain distinct orientations are present. The various components could therefore result from different numbers of misoriented nearest neighbors. For example, the a peak of $G_g(1)$ might result from a molecule with no misoriented neighbors, the b peak from one misoriented neighbor, and the c peak from two—other possibilities could account for the increased unresolved background in the fast quench spectrum.

We now return to the $A_g(2)$ line at ~ 1468 cm^{-1}, shown in Fig. 1. Of all the c-C_{60} lines, it is the only one for which the low temperature fine structure is found to be dominated by isotopic effects. The c-C_{60} and c-$^{12}C_{60}$ low T spectra are compared on an expanded energy scale in Fig. 4, revealing the great simplification present in the c-$^{12}C_{60}$ sample. In c-C_{60}, $A_g(2)$ has at least five components, indicated by the vertical ticks in the figure, at 1466.9, 1467.6, 1468.2, 1469.4, and 1470.8 cm^{-1}, while in c-$^{12}C_{60}$ only peaks at 1468.6 and 1470.8 cm^{-1} are observed (again, the strength of the $A_g(2)$ components makes their confusion with silent modes or combination modes unlikely).

The failure of the main c-$^{12}C_{60}$ peak to superimpose onto any of the c-C_{60} peaks is not an artifact, and must result from an interplay of isotopic and solid state effects. The situation is made even more clear by comparing the c-C_{60} spectrum with the spectrum of the same material dissolved in frozen CS_2, which except for lower resolution is identical to that recently published by Guha *et al.* [7]. There is absolutely no resemblance between the $A_g(2)$ spectrum of natural, crystalline C_{60} and natural C_{60} in CS_2 (the CS_2 spectrum can be readily understood on the basis of very simple arguments [7]). This again emphasizes the fact that in c-C_{60}, the isotopic effects are somehow strongly coupled to band structure effects, resulting in a spectrum quite different from that of the isolated molecule. Also

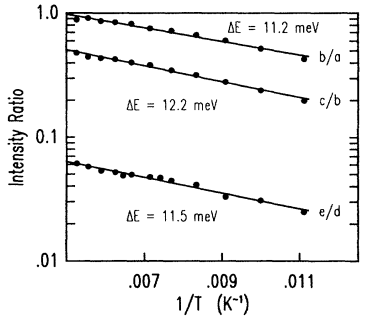

FIG. 3. Ratios of integrated intensities of the peaks labeled a, b, c, d, and e in Fig. 2 as a function of $1/T$. The solid lines are a fit to the data using the functional form $I_{\text{ratio}} = I_0 e^{-\Delta E/kT}$.

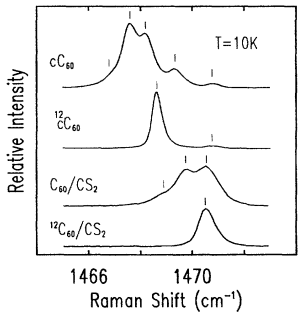

FIG. 4. Raman spectrum of the $A_g(2)$ mode of C_{60} single crystals (c-C_{60}), 97.3% $^{12}C_{60}$ single crystals (c-$^{12}C_{60}$), C_{60} dissolved in CS_2 (C_{60}/CS_2), and 97.3% $^{12}C_{60}$ dissolved in CS_2 ($^{12}C_{60}/CS_2$).

shown in Fig. 4 is the spectrum of pure $^{12}C_{60}$ in CS_2, revealing the expected single component at precisely the energy of the peak in the C_{60} sample attributed to $^{12}C_{60}$, and thus confirming the model of Guha *et al.* [7].

In conclusion, while we have been able to observe normal crystal field splittings both above and below the fcc to sc transition, we have found that the majority of the low temperature Raman fine structure is in fact related to the presence of merohedral disorder. Isotopic substitution in natural C_{60} plays a very minor role except for the $A_g(2)$ mode, which reveals a complicated isotopic structure entirely different from that of the isolated molecule, a phenomenon which merits further study.

This work was supported by the Natural Sciences and Engineering Research Council of Canada. We are indebted to Cambridge Isotope Labs for assistance in obtaining the ^{12}C enriched methane.

[1] H. W. Kroto *et al.,* Nature (London) **318**, 162 (1985).
[2] W. Krätschmer, K. Fostiropoulos, and D. R. Huffman, Chem. Phys. Lett. **170**, 167 (1990).
[3] P. H. M. van Loosdrecht *et al.,* Chem. Phys. Lett. **198**, 587 (1992).
[4] Z. H. Dong *et al.,* Phys. Rev. B **48**, 2862 (1993).
[5] K. A. Wang *et al.,* Phys. Rev B **48**, 11 375 (1993).
[6] M. Matus and H. Kuzmany, Appl. Phys. A **56**, 241 (1993).
[7] S. Guha *et al.,* Phys. Rev. Lett. **72**, 3359 (1994).
[8] P. A. Heiney, J. Phys. Chem. Solids **53**, 1333 (1992), and references therein.
[9] M. A. Verheijen *et al.,* Chem. Phys. Lett. **191**, 339 (1992).
[10] P. J. Horoyski and M. L. W. Thewalt, Phys. Rev. B **48**, 11 446 (1993).
[11] J. Yu, L. Bi, R. K. Kalia, and P. Vashishta, Phys. Rev. B **49**, 5008 (1994).
[12] R. C. Yu *et al.,* Phys. Rev. Lett. **68**, 2050 (1992).
[13] F. Gugenberger *et al.,* Phys. Rev. Lett. **69**, 3774 (1992).